DMD Fast Forward. Published on September 5, 2008 as doi:10.1124/dmd.108.022491

DMD #22491

Structural Determinants of Substrate Specificity Differences between Human Multidrug Resistance Protein (MRP) 1 (ABCC1) and MRP3 (ABCC3)

Caroline E. Grant, Mian Gao[1], Marianne K. DeGorter[2], Susan P.C. Cole, and Roger G. Deeley

Division of Cancer Biology and Genetics, Queen's University Cancer Research Institute, Kingston, ON, Canada (C.E.G., M.G., M.K.D., S.P.C.C., R.G.D.), Department of Pathology & Molecular Medicine (M.G., S.P.C.C., R.G.D.); Department of Biochemistry (R.G.D.)

Running title: Interaction of GSH and GSH-conjugates with MRP1

Address correspondence to: Roger G. Deeley, Division of Cancer Biology & Genetics, Queen's University Cancer Research Institute, Kingston, ON, Canada, K7L 3N6. E-mail: deeleyr@queensu.ca Number of text pages: 40

Number of tables: 2

Number of Figs: 8

Number of references: 42

Number of words in *Abstract*: 249

Number of words in *Introduction*: 750

Number of words in *Discussion*: 1,763

ABBREVIATIONS: MRP, multidrug resistance protein; ABC, ATP-binding cassette; MSD, membrane-spanning domain; TM, transmembrane helix; NBD, nucleotide-binding domain; SUR, sulfonylurea receptor; LTC_4, cysteinyl leukotriene C_4; $E_2$17ßG, estradiol-17ß-D-glucuronide; $E_1$3SO_4, estrone 3-sulfate; GSH, glutathione; MTX, methotrexate; SDS-PAGE, sodium dodecyl sulfate- polyacrylamide gel electrophoresis; MTT, 3-(4,5-dimethylthiazol-2-yl)-2,5-diphenyl tetrazolium bromide; mAb, monoclonal antibody; ß-gus, ß-glucuronidase

DMD Fast Forward. Published on September 5, 2008 as DOI: 10.1124/dmd.108.022491
This article has not been copyedited and formatted. The final version may differ from this version.

ABSTRACT

Multidrug Resistance Proteins (MRPs) are members of the 'C' branch of the ABC transporter superfamily. Human MRP1 transports a wide range of natural product drugs and structurally diverse conjugated and unconjugated organic anions. Its closest relative is MRP3. Despite their structural similarity, the homologs differ substantially in their substrate specificity. Notably, MRP1 transports glutathione (GSH) and GSH conjugates, and displays GSH stimulated transport of a number of unconjugated and conjugated compounds. In contrast, MRP3 does not transport GSH and is a poor transporter of GSH conjugates. However, both proteins transport glucuronide conjugates, such as 17β-estradiol 17-(β-D-glucuronide) ($E_2$17βG). We have constructed a series of MRP1/MRP3 hybrids and used them to identify a region of MRP1 that is critical for binding and transport of GSH conjugates such as leukotriene C_4 (LTC_4). Substitution of this region encompassing transmembrane helices 8-9 and portions of cytoplasmic loops 4 and 5 of MRP1 with the equivalent region of MRP3, eliminated LTC_4 transport. Transport of other substrates was either unaffected or enhanced. We identified three residues in this region, Tyr^{440}, Ile^{441} and Met^{443}, mutation of which differentially affected transport. Notably, substitution of Tyr^{440} with Phe, as found in MRP3, reduced LTC_4 and GSH-stimulated estrone-3-sulfate transport, without affecting transport of other substrates tested. The mutation increased the K_m for LTC_4 5-fold and substantially reduced photolabeling of MRP1 by both [^{3}H]LTC_4 and the GSH derivative, azidophenacyl-[^{35}S]GSH. These results suggest that Tyr^{440} makes a major contribution to recognition of GSH and the GSH moiety of conjugates such as LTC_4.

The ATP Binding Cassette (ABC) transporter, Multidrug Resistance Protein (MRP) 1 was identified in a human small cell lung cancer cell line, H69AR that exhibited cross resistance to a broad range of natural product type drugs (Cole et al., 1992). MRP1 was highly overexpressed in H69AR cells and, following gene transfer studies, was shown to cause a multidrug resistance (MDR) phenotype (Grant et al., 1994; Cole et al., 1994). MRP1 has since been found to be expressed in many solid tumors and hematological malignancies and in some, MRP1 is a negative prognostic indicator of treatment outcome (Deeley et al., 2006).

In vitro, MRP1 confers resistance to many structurally and functionally diverse natural product chemotherapeutic agents, including anthracyclines, *Vinca* alkaloids and epipodophyllotoxins. MRP1 also actively transports a range of glutathione (GSH)-, glucuronide- and sulfate-conjugated organic anions (Deeley et al., 2006). The GSH-conjugated, cysteinyl leukotriene C_4 (LTC_4) is the best characterized physiological substrate of MRP1 (Leier et al., 1994; Loe et al., 1996b). Other potential physiological substrates include the peptides, GSH and GSSG, the glucuronide conjugate, 17β-estradiol 17-(β-D-glucuronide) ($E_2$17βG) and the steroid sulfate, estrone 3-sulfate ($E_1$3SO_4) (Leier et al., 1994; 1996; Loe et al., 1996a; Qian et al., 2001b). MRP1 also transports chemotherapeutic agents to which it confers resistance, such as methotrexate (MTX), vincristine, daunorubicin and etoposide (VP-16) (Loe et al., 1996b; Rappa et al., 1997; Hooijberg et al., 1999; Renes et al., 1999). Transport of certain substrates, both unconjugated (e.g. vincristine and VP-16) and conjugated (e.g. $E_1$3SO_4), is stimulated by GSH (Loe et al., 1996b, 1998; Sakamoto et al., 1999; Qian et al., 2001b; Zelcer et al., 2003). In some cases (e.g. vincristine), the GSH-dependent substrate may reciprocally stimulate GSH transport while in others (e.g. $E_1$3SO_4) no stimulation is observed (Loe et al., 1998; Qian et al., 2001b).

MRP1 is a member of the 'C' branch of the ATP-binding cassette superfamily which includes the cystic fibrosis transmembrane conductance regulator (ABCC7), the two sulfonylurea receptors (SUR1/ABCC8, SUR2/ABCC9) and 8 other MRP1-related proteins (ABCC2-6 and 10-12/MRP2-6 and 7-9). Most ABC transporters are made up of two membrane spanning domains (MSD), each composed of 6 transmembrane (TM) helices and two cytosolic nucleotide binding domains (NBDs). However, MRPs 1, 2, 3, 6 and 7 and the two SURs have an additional relatively poorly conserved MSD, MSD0, that contains 5 TM helices and a glycosylated extracellular NH_2-terminal region (Deeley et al., 2006).

MRP1 is most closely related to MRP3 (58% identity) while the protein's substrate specificity is most similar to that of MRP2 (49% identity). MRP3 differs from MRP1 and MRP2 in both its drug resistance and conjugated anion transport profiles (Deeley et al., 2006). Like MRP1 and MRP2, MRP3 confers resistance to epipodophyllotoxins, such as etoposide, but not to *Vinca* alkaloids or anthracyclines (Kool et al., 1999; Zelcer et al., 2001; Zhang et al., 2003). MRP3 also transports certain glucuronide conjugates, including $E_2$17βG, that are MRP1 and MRP2 substrates, as well as other compounds which are not transported by the other two proteins (Zeng et al., 2000; Hirohashi et al., 2000; Zelcer et al., 2001; Zhang et al., 2003). Unlike MRP1 and MRP2, MRP3 does not transport GSH and the efficiency with which it transports GSH conjugates, such as LTC_4, is low (Zeng et al., 2000; Zelcer et al., 2001).

Site-directed mutagenesis studies have identified a number of residues that are either critical for overall activity or influence the substrate specificity of MRP1 but few have been identified that selectively affect transport of GSH-conjugates, such as LTC_4 (reviewed in Deeley et al., 2006). Two notable exceptions are Lys^{332} and His^{335} in TM6. Certain mutations of both residues reduce LTC_4 and apigenin-stimulated GSH transport without affecting transport of other

MRP1 substrates, such as $E_2$17ßG or MTX (Haimeur et al., 2002; 2004). However, these studies have also demonstrated that it is not possible to predict structure/substrate specificity relationships based on amino acid sequence conservation among MRP homologs, and that mutation of even exceptionally conserved amino acids can differentially and selectively affect the transport of shared substrates such as $E_2$17βG (reviewed in Deeley et al., 2006).

In the present study, we have used MRP1/MRP3 hybrid proteins to screen for regions, rather than individual amino acids, of MRP1 that are important for the transport of LTC_4 and other GSH-conjugates as a first step towards locating the critical residues involved. Using MRP1/MRP3 hybrids that covered all of MSD1 and MSD2, a region of MRP1 that includes TMs 8 and 9 (amino acids 425 to 516) was located which, when replaced with amino acids 411-502 of MRP3, completely eliminated LTC_4 transport while modestly enhancing transport of $E_2$17ßG. Within this region there are 26 amino acids that differ between the two proteins, among them we were able to identify a cluster of three residues in TM8, Tyr ^{440}, Ile^{441} and Met^{443} in MRP1 and Phe^{426}, Leu^{427} and Leu^{429} in MRP3, that contributes significantly to this major difference in substrate specificity between the two proteins.

Materials and Methods

Materials. [^{3}H]LTC$_4$ (165.7 Ci/mmol), [^{3}H]E$_2$17βG (45 Ci/mmol), [^{3}H]E$_1$3SO$_4$ (57.3 Ci/mmol) and [^{35}S]GSH (1498 Ci/mmol) were from Perkin Elmer Life Sciences (Boston, MA) and [^{3}H]MTX (28Ci/mmol) was from Moravek Biochemicals, Inc. (Brea, CA). Hygromycin, doxorubicin hydrochloride, etoposide (VP-16), vincristine sulfate, S-methyl GSH, the unlabelled equivalents of the tritiated compounds and the reagents for synthesis of azidophenacyl-[^{35}S]GSH were purchased from Sigma-Aldrich Chemical Co. (St. Louis, MO). Methotrexate was obtained from Faulding (Canada) Ltd. (Montreal, QC).

Cell Lines and Tissue Culture. HEK293 cells were grown Dulbecco's minimal essential medium plus 7.5% fetal bovine serum (Sigma) and Sf21 cells in Grace's medium supplemented with 0.2 % tryptose broth and 10% fetal bovine serum (Sigma). The HEK293 cell line transfected with the pCEBV7 vector, with and without the MRP1 coding sequence (HEK-MRP1 and PC7, respectively), have been described previously (Cole et al., 1994). The mutant MRP1 cDNAs were also cloned into the pCEBV7 vector and HEK293 cells were transfected using Fugene™ (Roche Applied Science, Laval, QC, Canada) according to the manufacturer's directions. After at least 2 weeks of selection in 100 μg/ml hygromycin, cloned cell lines were isolated by limiting dilution and tested for MRP1 expression.

Wild-type MRP1 was expressed in Sf21 insect cells as two half molecules, amino acids 1-932 and 932 -1531, using the Baculovirus expression vector pFASTBAC dual (Invitrogen, Carlsbad, CA) as previously described (Gao et al., 1996). Similarly, ß-glucuronidase (ß-gus) was expressed in Sf21 cells using the expression vector pFASTBAC. Generation of recombinant bacmids and baculoviruses and conditions for viral infection have also been described previously (Gao et al., 1996).

Hybrid cDNA Construction and Site-Directed Mutagenesis. To generate the vectors expressing the hybrid MRP1/MRP3 proteins, the relevant portions of MRP3 were amplified by polymerase chain reaction (PCR) using oligonucleotide primers with the appropriate MRP1 restriction enzyme cleavage sites added to the 5' ends. If the MRP3 fragment contained the cleavage site of choice, then a compatible cleavage site was used instead. Following cleavage of both the PCR fragment(s) and the appropriate vector containing a portion of the MRP1 cDNA, the DNA fragments (2 or 3) were ligated together. The identity of each construct was confirmed by restriction enzyme digestion and the fidelity of the PCR checked by sequencing. Finally, the MRP1/MRP3 hybrid portion of the construct was moved into the pFASTBAC dual-MRP1 expression vector.

To generate the vectors expressing the mutant MRP1 proteins, site-directed mutagenesis was performed using the QuikChange® II Site-Directed Mutagenesis Kit (Stratagene, La Jolla, CA). The target sequence for the PCR was an approximately 2.7 kb 5' end of MRP1 cDNA cloned into the pGEM3Zf^{+} vector (Fisher Scientific, Pittsburgh, PA). Following sequencing to ensure the fidelity of the PCR, the MRP1 fragment was cloned into pFASTBAC dual containing wild-type MRP1, replacing the equivalent un-mutated fragment. Similarly, a Bgl II fragment from the pFASTBAC dual clone containing the mutant MRP1 cDNAs was moved into the mammalian expression vector, pCEBV7-MRP1. Each construct was verified to be correct by both sequencing and restriction enzyme analysis.

Determination of Relative MRP1 Protein Levels. Membrane vesicles were prepared from either Sf21 or HEK293 cells by nitrogen cavitation followed by layering on a 35% sucrose cushion as previously described (Loe et al., 1996b). Total membrane protein concentration was determined by Bradford assay (Bio-Rad, Mississauga, ON, Canada) and then serially diluted

DMD Fast Forward. Published on September 5, 2008 as DOI: 10.1124/dmd.108.022491
This article has not been copyedited and formatted. The final version may differ from this version.

protein samples from each membrane preparation was analysed either in sodium dodecyl sulfate-polyacrylamide gel electrophoresis (SDS-PAGE), followed by electroblotting to Immobilon-P membranes (Millipore, Bedford , MA), or transferred to the same membrane using a Bio-dot SF microfiltration apparatus (Bio-Rad). In each case, the appropriate wild-type MRP1, either the full-length protein or protein expressed as two half-molecules, was included on each blot. The membranes were probed using anti-MRP1 monoclonal antibodies (mAb) MRPm6, MRPr1 (Alexis Biochemicals, San Diego, CA) and QCRL-1 (Hipfner et al., 1996), and antibody binding detected using horseradish peroxidase-conjugated goat anti-mouse or anti–rat IgG (Pierce Biotechnology, Rockford, IL), enhanced chemiluminescence detection and X-Omat Blue XB-1 film (PerkinElmer Life Sciences, Boston, MA). Densitometry of the film images was performed using a ChemiImager 4000 (Alpha Innotech Corp., San Leandro, CA) or a ScanMaker i900 scanner (Microtek, Carson, CA) and Photoshop 5.5 software (Adobe Systems, Ottawa, ON, Canada). Either multiple blots or multiple exposures of the same blot were used to analyze the relative MRP1 protein levels. Expression of each protein was determined relative to wild-type MRP1 and the transport levels normalized accordingly. For proteins expressed as half molecules, the levels of expression of each half molecule as compared to the equivalent wild-type fragment were determined. In some cases, the half molecules of the mutant protein were expressed within ± 10% of the wild-type fragments. In this case, no normalization was done. Where expression of the mutant protein differed more substantially, normalization was done using the expression levels of the least abundant half molecule compared to its wild-type counterpart.

Transport of ^{3}H-Labeled Substrates into Membrane Vesicles. Plasma membrane vesicles were prepared as described previously and ATP-dependent transport into inside-out membrane vesicles was measured using a rapid filtration technique (Loe et al., 1996b). LTC_4

DMD Fast Forward. Published on September 5, 2008 as DOI: 10.1124/dmd.108.022491
This article has not been copyedited and formatted. The final version may differ from this version.

transport assays were performed at 23°C, in a 20 µl reaction volume containing 2-4 µg of membrane vesicle protein, 50 nM [^{3}H]LTC_4 (20 nCi per reaction), 10 mM $MgCl_2$, 4 mM ATP or AMP, in transport buffer (250 mM sucrose, 50 mM Tris.HCl pH 7.5). ATP-dependent uptake was calculated by subtracting the uptake in the presence of AMP from the uptake measured in the presence of ATP. The results are expressed as means ± SD of triplicate determinations in each assay.

Uptake of [^{3}H]$E_2$17βG was measured in a comparable fashion except that transport was measured at 37°C in a reaction containing 400 nM [^{3}H]$E_2$17βG (40 nCi per reaction). [^{3}H]MTX uptake was also measured at 37°C for 20 min in a reaction mixture containing 100 µM [^{3}H]MTX (200 nCi per reaction). [^{3}H]$E_1$3SO_4 uptake was measured at 37°C at a final concentration of 6 µM [^{3}H]$E_1$3SO_4 (80 nCi per reaction) with the addition of 2 mM S-methyl GSH.

K_m and V_{max} values of ATP-dependent [^{3}H]LTC_4 uptake in membrane vesicles (4 µg) were measured at 6-7 LTC_4 concentrations (25 nM - 1 µM) for 1 min at 23°C in transport buffer containing 4 mM AMP or ATP and 10 mM $MgCl_2$. Data were analysed using Graph Pad Prism™ software, and kinetic parameters determined by linear regression analysis of a Hanes-Wolff plot. Similarly, initial rates of [^{3}H]$E_1$3SO_4 uptake was measured as described for LTC_4 except that the assay was done at 37ºC using a 30 sec time point and concentrations of $E_1$3SO_4 ranging from 3-20 µM, as described above.

Photoaffinity Labeling of Wild-type and Mutant MRP1 Proteins with [^{3}H]LTC_4. Samples containing approximately equivalent levels of MRP1 protein were mixed in a 30 µl reaction volume and an aliquot (2 µl) removed. The remaining 28 µl was then mixed with [^{3}H]LTC_4 (200 nM, 0.13 µCi) and incubated for 30 min at room temperature. After freezing in liquid N_2, samples were cross-linked at 302 nm for 1 min as described previously (Loe et al.,

DMD Fast Forward. Published on September 5, 2008 as DOI: 10.1124/dmd.108.022491
This article has not been copyedited and formatted. The final version may differ from this version.

1996b). The freezing and cross-linking cycle was repeated nine more times. Both the cross-linked and native proteins (the 2 µl sample) were resolved by electrophoresis through 5-15% gradient SDS-polyacryamide gels. The gel containing the cross-linked proteins was fixed, processed for fluorography by soaking in Amplify (GE Healthcare, Baie d'Urfé, QC, Canada), dried and then exposed to film for approximately 2 weeks. The non-radioactive gel was processed as described for immunoblots above.

Preparation of Azidophenacyl-[^{35}S]GSH and Photolabeling of Wild-type and Mutant MRP1 Proteins. Azidophenacyl-[^{35}S]GSH was prepared essentially as described previously except that 100 µCi of [^{35}S]GSH (1498 Ci/mmol) was diluted to approximately 500 Ci/mmol with cold GSH (Qian et al., 2002). For photolabeling, HEK293 membrane vesicles containing approximately equivalent amounts of wild-type or mutant MRP1 protein were mixed with membrane vesicles from the control cell line, PC7, such that each sample contained 120 µg of total membrane protein in 60 µl of transport buffer. A sample (4 µg) was taken before photolabeling for immunoblot analysis, as described for [^{3}H]LTC_4 photolabeling. Each sample was then incubated with 0.25 µCi of azidophenacyl-[^{35}S]GSH at room temperature for 10 min and irradiated at 312 nm on ice for 5 min. The membrane vesicles were collected by centrifugation at 14000 rpm for 15 min before solubilization in 50 mM Tris pH 7.5 and Laemmli buffer. After resolving the proteins in 6% SDS-PAGE, the gel was treated with Amplify for 20 min, dried and exposed to film with an intensifying screen for up to 3 days.

Chemosensitivity Testing. Drug resistance was determined using a colorimetric 3-(4,5-dimethylthiazol-2-yl)-2,5-diphenyl tetrazolium bromide (MTT) assay as described previously (Cole et al., 1994). Mean values ± SD of quadruplicate determinations were plotted using Graphpad software. IC_{50} values were obtained from the best fit of the data to a sigmoidal curve.

Relative resistance is expressed as the ratio of the IC_{50} values of cells expressing mutant or wild-type MRP1 compared to cells containing the empty expression vector. Resistance values were the average of 3 or more independent experiments.

Results

Identification of Regions in MRP1 and MRP3 Responsible for Differences in LTC_4 Transport.

Based on the relatively high amino acid sequence identity and similar predicted topology of MRP1 and 3 (Fig. 1A), 12 hybrid expression vectors were constructed such that limited regions of MSD1 and MSD2 of MRP1 were replaced with the predicted equivalent from MRP3 (Fig. 1B). Since we and others have shown previously that the MSD0 region of MRP1, defined here as amino acids 1-203, is not required for transport of a number of substrates, including LTC_4, this region was not included in our analysis (Bakos et al., 1998; Westlake et al., 2003). Each hybrid protein was expressed in Sf21 cells as an NH_2-terminal fragment of amino acids 1-932 and a COOH-terminal fragment of amino acids 932-1531 (Fig. 1B). When co-expressed these two fragments of wild-type MRP1 associate correctly and support ATP-dependent LTC_4 transport with an efficiency of approximately 90% compared with the intact protein (Gao et al., 2000). After preparation of membrane vesicles, the ability of each of the hybrid proteins to transport LTC_4 and $E_2$17βG was compared (data not shown). None of the constructs supported LTC_4 transport with the notable exception of constructs C and J which displayed transport activity similar to, or approximately 50% of, wild-type levels, respectively. Construct C contained four of the six TMs of MSD2 from MRP3 (TMs 12-15) while construct J contained only TMs 12 and 13 of MRP3. Neither of these constructs transported $E_2$17βG, nor did constructs A, E, F, H, K and L, although a low level of transport was detected with constructs B, D and I. The only construct that retained $E_2$17βG transport activity while losing the ability to transport LTC_4 was construct G, in which amino acids 425-516 in MSD1 of MRP1 (TMs 8 and 9) were replaced with amino acids 411-502 of MRP3 (Fig. 1B). The G construct actually showed enhanced $E_2$17βG (Fig. 1D) transport compared to wild-type MRP1 while LTC_4 transport was

reduced to approximately 15% of wild-type levels (Fig. 1C). This observation, coupled with the ability to exchange four TMs of MSD2 of MRP1 for those of MRP3 without loss of LTC_4 transport (construct C), strongly suggested that the region encompassing TMs 8 and 9 of MRP1 contained non-identical residues that were critical for LTC_4 binding and/or transport.

To determine if a smaller region of MRP1 could be exchanged with MRP3 and produce a similar effect on transport, hybrid constructs G1 (substitution of amino acids 425-477 of MRP1 with amino acids 411-463 of MRP3) and G2 (substitution of amino acids 478-516 of MRP1 with amino acids 464-502 of MRP3) were made (Fig. 2A), and the level of expression in Sf 21 cells (Fig. 2B) and transport of LTC_4 and $E_2$17βG were determined (Fig. 2C and D). LTC_4 transport by the G1 construct was approximately 40% of wild-type levels (Fig. 2C) while $E_2$17βG transport was 2 times the level obtained with wild-type MRP1 (Fig. 2D). For the G2 construct, LTC_4 transport was reduced by 80% (Fig. 2C) but $E_2$17βG transport was similar to wild-type MRP1 (Fig. 2D). Thus, both halves of the G region contain residues that alone or in concert affect LTC_4 transport by MRP1, whereas $E_2$17βG transport was either unchanged or enhanced by introduction of corresponding non-identical amino acids from MRP3.

Analysis of the Contribution of Non-identical Amino Acids in the G Region of MRP1 and MRP3 to LTC_4 and $E_2$17βG Transport. The results obtained with the hybrid proteins indicated that multiple residues throughout this region could contribute to interactions with LTC_4. Within the G region, there are 26 amino acid differences between MRP1 and MRP3 (Fig. 2A). Using site-directed mutagenesis, we attempted to identify those non-identical amino acids that had a major and selective effect on LTC_4 transport. Each of the 26 non-identical amino acids in MRP3 was introduced into MRP1, either as single residue substitutions, or as double substitutions where adjacent residues were involved. Constructs were expressed in Sf 21 cells

and after determining their expression levels (Fig. 3A), LTC_4 and $E_217\beta G$ transport was assessed for each mutant protein. In a preliminary screen based on single time point assays, the majority of individual, single mutations had negligible effect on LTC_4 transport (data not shown). The most dramatic reduction in transport was found for one double mutation located in the G1 region, Y440F/I441L, which reduced LTC_4 transport to less than 20% of wild-type levels (Fig. 3B). However, this double mutation also decreased $E_217\beta G$ transport to approximately 25% of wild-type MRP1 (Fig. 3C). A second double mutation, A481G/V482A, located in the G2 region also reduced LTC_4 transport by 6-fold and, in this case, $E_217\beta G$ transport was reduced to approximately a third of wild-type MRP1 levels (data not shown).

Since no single- or double-substituted mutant was found that alone explained the dramatic reduction in LTC_4 transport by the G hybrid protein while leaving $E_217ßG$ transport intact, a series of multiple mutations were made predominantly targeting clusters of non-identical amino acids (Table 1). With the exception of one triple mutation, in which substitution of M443 with L was introduced into the LTC_4 transport deficient Y440F/I441L double mutant, no combination of mutations tested reduced LTC_4 transport by more than 60-70% (data not shown). The Y440F/I441L/M443L virtually eliminated LTC_4 transport (Fig. 3B), but also reduced $E_217\beta G$ transport by approximately 80% (Fig. 3C).

Transport of LTC_4, $E_217\beta G$, E_13SO_4 and MTX by Y440F, I441L and M443L MRP1 Mutant Proteins. To further characterize the effects of the double and triple mutations on substrate specificity, we investigated the influence of individual contributing amino acid substitutions on transport of LTC_4 and $E_217\beta G$ as well as two additional substrates, E_13SO_4 and MTX. These two organic anion substrates were chosen because the former is transported by

MRP1 in a GSH- (or S-methyl GSH-) stimulated manner, but is not a substrate for MRP3, while MTX is transported by both proteins (Deeley et al., 2006).

The Y440F and M443L mutations each independently decreased initial rates of LTC_4 transport by approximately 60% and 50%, respectively, while the I441L mutation had little or no effect (Fig. 3B). In contrast, $E_2$17βG transport was decreased approximately 50% by both the I441L and M443L mutations, but only 20% by the Y440F mutation (Fig. 3C). All three mutations significantly decreased $E_1$3SO_4 transport in the presence of 2 mM S-methyl GSH, with the Y440F, I441L and M443L mutations reducing transport at 1 min by approximately 65%, 50% and 90%, respectively (Fig. 3D). However, none of the single mutations, nor the double-mutation, had a statistically significant effect on transport of the common MRP1/MRP3 substrate MTX (Fig. 3E). Thus mutation of each of these three amino acids differentially affects substrate specificity as opposed to overall transport activity, strongly suggesting that they are not simply perturbing the conformation of the protein and that they contribute to substrate recognition.

Kinetic Parameters of [^{3}H]LTC_4 Transport by Y440F and I441L Single and Double Mutants. We also determined the effects of the Y440F and I441L single and double mutations on the K_m and V_{max} for LTC_4 transport. The K_m and V_{max} values obtained for wild-type MRP1 were 72 nM and 37 pmol mg^{-1} min^{-1}, respectively, while the K_m for the Y440F mutation was 328 nM and the normalized V_{max}, was 41 pmol mg^{-1} min^{-1} (Fig. 4A and B). The increase in K_m suggested that the relatively conservative substitution of Phe for Tyr results in an almost 5-fold decrease in apparent affinity for LTC_4 with no change in the maximum rate of transport. Although LTC_4 transport by the I441L mutant was only marginally decreased at a fixed concentration of substrate, linear regression analysis indicated that the K_m for LTC_4 was increased approximately 2-fold (149 nM for the I441L mutant protein vs. 72 nM for wild-type

DMD Fast Forward. Published on September 5, 2008 as DOI: 10.1124/dmd.108.022491
This article has not been copyedited and formatted. The final version may differ from this version.

MRP1), again with no significant change in V_{max} (normalized V_{max} for the I441L mutation 42 pmol mg^{-1} min^{-1} vs. 37 pmol mg^{-1} min^{-1} for the wild-type protein) (Fig. 4A and B). Transport of LTC_4 by the double mutant was markedly reduced compared to either of the single mutations alone. As a consequence, it was technically impossible to determine an accurate K_m for LTC_4.

Photolabeling of the NH_2- and COOH-terminal Halves of MRP1 Mutant Proteins by LTC_4. To confirm whether or not the increase in K_m resulting from the Y440F mutation reflected a decreased affinity for substrate, we examined the effect of the mutation on photolabeling of MRP1 with [^{3}H]LTC_4. Based on the expression levels of the 3 mutant proteins relative to wild-type MRP, the quantity of membrane vesicles used for photolabeling was adjusted to yield equivalent amounts of wild-type or mutant MRP1 in each photolabeled sample. To confirm that this was achieved, an aliquot of each protein sample used for photolabeling was reexamined by SDS-PAGE, immunoblotting and densitometry (Fig. 5A).

Previously, we have shown that LTC_4 binds to both NH_2- and COOH-terminal fragments of MRP1 asymmetrically (Qian et al., 2001a). As shown in Fig. 5B, [^{3}H]LTC_4 predominantly labels the NH_2-terminal fragment containing amino acids 1-932 of wild-type MRP1, although labeling of the COOH-terminal fragment, amino acids 932-1531, was still readily detectable. Photolabeling of both fragments of the I441L mutant protein, which displayed only a 2-fold increase in K_m, was essentially indistinguishable from that obtained with the wild-type MRP1 protein. However, photolabeling of the NH_2-terminal fragments of both the Y440F and double Y440F/I441L mutant proteins was similarly, substantially reduced compared with both the wild-type and the I441L mutant. These data are consistent with the results of kinetic studies and strongly support the suggestion that theY440F mutation results in a substantial decrease in affinity for LTC_4. Furthermore, photolabeling of the COOH-terminal fragment of the Y440F and

DMD Fast Forward. Published on September 5, 2008 as DOI: 10.1124/dmd.108.022491
This article has not been copyedited and formatted. The final version may differ from this version.

Y440F/I441L mutant proteins was also reduced when compared to wild-type MRP1 or the I441L mutant, despite the fact that this region is identical in all four proteins. Thus, photolabeling of the NH_2- and COOH-proximal halves of the protein appears not to be the result of interaction of LTC_4 with two functionally independent sites.

Mutational Analysis of Residue Y440. We next examined the functional consequences of less conservative substitutions of Tyr^{440}. These included non-aromatic neutral (Ala), polar (Ser), polar neutral (Gln) and acidic (Glu) residues, as well as a polar aromatic substitution with Trp. Vesicles containing the mutant proteins were then tested for their ability to transport LTC_4. All of these mutations had a greater effect on transport than the more conservative Y440F mutation. Transport by the two polar mutations Y440Q and Y440S was decreased by 75-80%, while the charged and neutral mutations decreased transport by more than 90% (Fig. 6A). To determine whether the size of the aromatic side chain was critical, as well as its polarity, we created a Tyr to Trp mutation. This mutation decreased LTC_4 transport by 75% compared to the wild-type protein (Fig. 6A). In addition, unlike the Y440F mutation which had little effect on $E_217\beta G$ transport, the Y440W mutation essentially eliminated transport of the conjugated estrogen (Fig. 6B).

Kinetic Parameters of S-methyl GSH-stimulated [^{3}H]Estrone 3-Sulphate Transport and Azidophenacyl[35S]-GSH Photolabeling of Wild-type and Mutant MRP1 Proteins. The Y440F mutation has a major deleterious effect on the transport of LTC_4 and the S-methyl GSH-stimulated transport of E_13SO_4 (Fig. 3B and D), but not the other estrogen conjugate tested ($E_217ßG$) or MTX (Fig. 3C and E). Since we have shown that the Y440F mutant protein has reduced affinity for LTC_4 compared to wild-type MRP1 (Fig. 4B), it is possible that the Y440F mutation also affects the affinity for E_13SO_4 and/or S-methyl GSH. To test the former

DMD Fast Forward. Published on September 5, 2008 as DOI: 10.1124/dmd.108.022491
This article has not been copyedited and formatted. The final version may differ from this version.

hypothesis, we attempted to determine a K_m for the transport of E_13SO_4 by wild-type MRP1 and the Y440F mutant. Unfortunately, the levels of transport by the mutant precluded determination of a reliable K_m. However, the transport deficiency showed no indication of being overcome by using concentrations of E_13SO_4 as much as 10-fold higher than the K_m of wild-type MRP1 in transport assays (Fig. 7A). Thus, although we were unable to determine whether K_m was affected, it appears likely that the mutation decreases the V_{max} for E_13SO_4 transport possibly as a result of decreasing the affinity for S-methyl GSH.

To test whether the Y440F mutation alters the binding characteristics of S-methyl GSH and thus E_13SO_4 transport, we examined the binding of a GSH analogue, azidophenacyl-GSH, to wild-type and mutant MRP1 expressed in stably-transfected HEK cells. We have previously shown that this analogue can substitute for GSH or S-methyl GSH in stimulating E_13SO_4 transport and, when radiolabelled with ^{35}S, binds to MRP1 in a fashion similar to that found for LTC_4 (Qian et al., 2002). The M443L mutation reduced S-methyl GSH-stimulated E_13SO_4 transport by 90% in Sf21 cells (Fig. 3D). As shown in Fig. 7B and C, binding of azidophenacyl-[^{35}S]GSH by this mutant protein was barely detectable when compared to wild-type MRP1, despite the use of almost 2-fold more mutant than wild-type protein in the samples shown. Thus, the affinity for azidophenacyl-GSH is severely affected by the M443L mutation. In contrast, the I441L mutant protein which decreased S-methyl GSH-stimulated transport of E_13SO_4 by 55% compared to wild-type MRP1 (Fig. 3D), bound approximately equivalent levels of azidophenacyl-[^{35}S]GSH (Fig. 7C), suggesting that, as was determined for LTC_4, the affinity for azidophenacyl-GSH is relatively unaffected by the I441L mutation. In contrast, the Y440F mutation which reduced S-methyl GSH-stimulated transport of E_13SO_4 by approximately 65% (Fig. 3D) markedly decreased photolabeling with azidophenacyl-[^{35}S]GSH (Fig. 7C). This

suggests that the affinity for this GSH derivative is dramatically affected by the Y440F mutation, as was found for LTC_4. The reduced affinity for both azidophenacyl GSH and LTC_4 suggests that the Y440F mutation may alter the interaction of MRP1 with the GS-moiety of both compounds and thus may decrease E_13SO_4 transport by reducing the affinity for GSH and S-methyl GSH.

Effect of the Y440F, I441L, M443L and Y440F/I441L Mutations on Resistance to Vincristine, Doxorubicin and VP-16. Lastly, the drug resistance profiles of Y440F, I441L, M443L and Y440F/I441L mutant proteins were examined since unlike MRP1, the profile of resistance to natural product drugs conferred by MRP3 is restricted primarily to epipodophyllotoxins (Deeley et al., 2006). Each single and the double mutant protein was stably expressed in cloned populations of HEK293 cells and the subcellular localization of wild-type and mutant MRP1s was compared by immunostaining with the MRP1-specific mAb MRPm6 and confocal microscopy to ensure that none of the mutations adversely affected protein trafficking (see supplemental data).

Cells expressing MRP3 were significantly resistant to VP-16 (6.4-fold) but not to either Vincristine (1.1-fold) or Doxorubicin (0.87-fold), while cells expressing wild-type MRP1 were resistant to all three classes of drugs (15.6-fold, 16.2-fold and 4.5-fold for Vincristine, VP-16 and Doxorubicin, respectively), consistent with previous results (Table 2) (Grant et al., 1994; Cole et al., 1994; Kool et al., 1999; Zelcer et al., 2001; Zhang et al., 2003). The three single mutations each decreased resistance to Vincristine and VP-16, 2- to 3-fold, while only the Y440F mutation resulted in a major decrease in resistance to Doxorubicin. The effect of the double Y440F/I441I mutation appeared to be additive with respect to both VP-16 and Doxorubicin resistance, but resulted in no greater decrease in resistance to Vincristine than either mutation alone. Thus, as

observed during organic anion transport studies, each mutation had different effects on the drug resistance profile of MRP1, suggesting that all three of these residues contribute to recognition of natural product drugs, as well as the organic anion substrates tested. However, none of the mutations resulted in a profile more closely resembling that of MRP3.

Discussion

In studies described here, we sought to identify additional residues involved in the binding and transport of GSH and GSH conjugates by MRP1. We did so by constructing a series of MRP1/MRP3 hybrids and searching for regions which when exchanged decreased transport of the high affinity MRP1 substrate, LTC_4, without affecting transport of the shared substrate, $E_2$17ßG. The approach was based on the premise that such regions would contain amino acids that differ between MRP1 and MRP3 which are determinants of LTC_4 specificity. We found that it was possible to exchange most of MSD2, encompassing TMs 12-15, with little effect on LTC_4 transport. This observation, together with previous studies showing that point mutations in TMs 16 and 17 have little effect on LTC_4 transport by MRP1, suggested that non-identical residues critical for LTC_4 transport were localized in MSD1 and possibly the cytoplasmic linker region (CL3) (Deeley et al., 2006). The only hybrid that displayed a major, selective decrease in LTC_4 transport contained amino acids 411-502 of MRP3 in place of amino acids 425-516 of MRP1. Exchange of this region, spanning TMs 8 and 9, completely eliminated LTC_4 transport with little effect on transport of $E_2$17βG. Four amino acids in this region of MRP1, Arg^{433}, Asp^{436}, Trp^{459} and Pro^{478}, have been shown previously to be determinants of the substrate specificity of MRP1 (Koike et al., 2002; Conrad et al., 2002; Haimeur et al., 2004; Koike et al., 2004). Mutation of three them, Arg^{433}, Asp^{436} and Pro^{478}, affects transport of LTC_4. Arg^{433} and Asp^{436} are predicted to be located in a cytoplasmic helical region that is an extension of TM8, while Pro^{478} is located within TM9. However, all of these residues are identical between MRP1 and MRP3 and thus would not be revealed by the approach we have taken.

The G region contains 26 amino acids that differ between MRP1 and MRP3. Analysis of hybrids containing sub-fragments spanning either TM 8 or TM 9 suggested that multiple non-

identical residues were likely to contribute to LTC_4 specific transport. Consequently, we were unable to completely replicate the results of exchanging the entire region, by mutating the 26 non-identical amino acids singly, or as clusters of up to eight residues. Furthermore, individual mutation of many of these residues had negligible effects on transport of any of the substrates tested. This result is consistent with current models of the interaction of multidrug transporters with their structurally diverse substrates which is believed to involve multiple, often overlapping, weak interactions between the ligand and a relatively large and flexible binding pocket or surface (reviewed in Deeley and Cole, 2006). However, we did locate a trio of non-identical amino acids predicted to be in the inner leaflet region of TM8, each of which selectively affected the substrate specificity of MRP1. Notably, conservative substitution of Tyr^{440} with Phe as present in MRP3, reduced LTC_4 transport by ~60% with little effect on transport of $E_2$17βG. This mutation also reduced transport of the GSH-dependent MRP1 substrate $E_1 3SO_4$, but not the unconjugated organic anion MTX, which is transported by both MRP1 and MRP3 (Deeley et al., 2006).

The Y440F mutation resulted in a significant decrease in the apparent affinity for LTC_4 (4-5 fold increase in K_m) while V_{max} was not affected. In addition, photolabeling of the Y440F protein by [^{3}H]LTC_4 was markedly decreased. Taken together, the data strongly suggested that the primary defect in the Y440F protein was at the level of LTC_4 binding. Sequence comparison with the human MRP family (Fig. 2A) revealed that seven of nine members have Tyr or Phe at the position corresponding to MRP1 Y440. Thus the presence of an aromatic amino acid at this position is relatively highly conserved across family members and may be of broad functional importance for substrate recognition. In addition to MRP1, MRP6 and the more distantly related MRP4 have been shown to transport LTC_4 with relatively high affinity (Illias et al. 2002, Rius et al. 2008). However, while Y440 is conserved in MRP6, the corresponding residue in MRP4 is

Phe, as it is in MRP3. The lack of complete conservation among the LTC4 transporters is not unexpected. Extensive studies have shown that structure/substrate specificity relationships cannot be predicted based on amino acid sequence conservation among MRP homologs, and that even exceptionally conserved amino acids do not necessarily make the same contributions to recognition of common substrates (reviewed in Deeley et al., 2006).

Other conservative (W) and non-conservative (A, E, Q and S) substitutions of Y440 caused significant reductions in LTC_4 transport ranging from 75% (Y440Q) to 90% (Y440A and Y440E). In particular, the relatively conservative substitution with Trp not only decreased LTC_4 transport by ~75%, but unlike the Y440F mutation, essentially eliminated transport of $E_2$17βG. Thus, it appears that both the size and the polarity of the aromatic side chain at this location are important for the interaction of MRP1 with LTC_4, while it is primarily the size that is critical for interaction with $E_2$17ßG. Whether the mutations exert their effects by altering direct contacts between substrate and the mutated residue, or by localized perturbations in regions of the binding pocket important for interaction with certain substrates and not others is presently not known.

In contrast to the Y440F mutation, the conservatively substituted I441L mutation had no effect on LTC_4 or MTX transport but decreased transport of both $E_2$17ßG and $E_1$3SO_4, while the M443L mutation decreased transport of all three conjugated substrates but not MTX. Similarly, mutation of each of these three residues caused differential effects on the drug resistance profile of MRP1, consistent with their importance in determining recognition and transport of a number of substrates in addition to LTC_4. As suggested previously, these observations are compatible with the existence of a common binding pocket with each substrate establishing multiple overlapping but not identical interactions with the protein (Deeley et al., 2006).

The clustering of Tyr^{440}, Ile^{441} and Met^{443}, in a single turn of TM8 is similar to that of three previously identified mutation-sensitive residues in TM6, Lys^{332}, His^{335} and Asp^{336}. Mutations of Lys^{332} and His^{335} affect substrate specificity in a similar and selective fashion while mutation of Asp^{336} affects overall transport activity (Haimeur et al., 2002; 2004;). Most significantly, the conservative substitution of Lys^{332} by Arg increased the K_m for LTC_4 ~5-fold without affecting the V_{max}, as is the case with the Y440F mutation. Other non-conservative mutations of Lys^{332} abrogated LTC_4 transport, as was observed with certain non-conservative substitutions of Tyr^{440}. In addition, photolabeling with [^{3}H]LTC_4 of K332D and K332L mutant proteins was severely reduced compared to wild-type MRP1. Thus, mutations of both TM6-Lys^{332} and TM8-Tyr^{440} decrease LTC_4 binding and both the charge (or polarity) and volume of the residue at either location is critical for interaction with LTC_4.

The Y440F mutation had little effect on either $E_2$17βG or MTX transport, but markedly decreased S-methyl GSH-stimulated $E_1$3SO_4 transport and photolabeling with the GSH analogue azidophenacyl-[^{35}S]GSH was severely reduced. Because of the magnitude of the effect, we were unable to determine the kinetic parameters of $E_1$3SO_4 transport. However, it is clear that the Y440F mutation almost entirely eliminates binding of azidophenacyl-GSH, as well as LTC_4. Since both S-methyl GSH and azidophenacyl-GSH can substitute for GSH in transport of $E_1$3SO_4 (Qian et al., 2002; Leslie et al., 2003), Tyr^{440} may interact with the GSH moiety of LTC_4, S-methyl GSH and azidophenacyl-GSH and thus reduce transport of both LTC_4 and $E_1$3SO_4. Consistent with this suggestion, the Y440F mutation resulted in a major decrease in resistance to all three classes of drugs, transport of, or resistance to which, has been shown to be GSH dependent (Loe et al., 1996b; Rappa et al., 1997; Loe et al., 1998; Renes et al., 1999).

Previously, we have used molecular modeling to examine possible spatial relationships among residues that affect the substrate specificity of MRP1, as well as the disposition of specific amino acid side chains with respect to the putative translocation pathway of the protein (Campbell et al., 2004; Deeley et al., 2006). The models of MRP1 and several other ABC transporters were based on the crystal structure of MsbA published by Chang and co-workers (2003). This structure differs significantly from that determined more recently for the *S. aureus* multidrug ABC transporter, Sav1866, and was retracted because of major errors in the packing and tilt of a number of TM's (Dawson and Locher, 2006; Chang et al., 2006; Dawson et al., 2007). Consequently, we developed a revised model based on the more recent Sav1866 structure (DeGorter et al., 2008). However, this structure corresponds to the ADP-trapped form of Sav1866 in which the protein is thought to be in its low-affinity substrate binding state, with the putative translocation pathway open to the extracellular side of the membrane. In such a configuration, it is presumed that the high-affinity site is occluded and inaccessible to substrate in the cytoplasm or membrane. Three views of this model are shown in Fig. 8 illustrating the predicted locations of residues in TM8 which when mutated selectively affect substrate specificity, in relation to those previously identified in TM6 which also differentially influence transport of LTC_4.

The TMs in the Sav1866-based structure are tilted relative to the likely translocation pathway, rather than being parallel to it and several of the helices display significant curvature (Fig. 8B) (DeGorter et al., 2008). For example, TM6 and TM8 are adjacent to each other and closely aligned in the inner leaflet region of the membrane, but tilt away from each other in the outer leaflet. The cluster of residues we have identified is located in the inner leaflet of the membrane with the side chains of Tyr^{440} and Ile^{441} aligned tangentially to the translocation

pathway while Met^{443} projects into it. In TM6, the previously identified residues are predicted to be located in the outer leaflet with Lys^{332} and Asp^{336} projecting into the 'open' end of the pathway. It has been proposed that changes in the conformation of the NBDs upon binding and release of nucleotide are transmitted to the MSDs *via* two coupling helices in each MSD, one of which (helix 1) interacts with both NBDs in the closed configuration, while the other (helix 2) interacts with the apposing NBD. In MSD1 of MRP1, coupling helix 1 is predicted to connect TM7 and TM8. Thus, one or both of these helices appear likely candidates for transmitting conformational changes induced by movement of coupling helix 1. It remains to be determined to what extent such a conformational change affects the accessibility of the residues in TM8, such as Tyr^{440} and Ile^{441} to hydrophilic substrates such as LTC_4 and GSH.

Acknowledgements

The authors wish to thank Heng-Ran Cui, Ruth Burtch-Wright and Monika Vasa for their excellent technical assistance.

References

Bakos E, Evers R, Szakacs G, Tusnady GE, Welker E, Szabo K, de Haas M, van Deemter L, Borst P, Varadi A and Sarkadi B (1998) Functional multidrug resistance protein (MRP1) lacking the N-terminal transmembrane domain. *J Biol Chem* 273:32167-32175.

Campbell JD, Koike K, Moreau C, Sansom MS, Deeley RG and Cole SPC (2004) Molecular modeling correctly predicts the functional importance of Phe594 in transmembrane helix 11 of the multidrug resistance protein, MRP1 (ABCC1). *J Biol Chem* 279:463-468.

Chang G (2003) Structure of MsbA from Vibrio cholera: a multidrug resistance ABC transporter homolog in a closed conformation. *J Mol Biol* 330:419-430.

Chang G, Roth C.B., Reyes CL, Pornillos O, Chen Y-J and Chen AP (2006) Retraction. *Science* 314:1875.

Cole SPC, Bhardwaj G, Gerlach JH, Mackie JE, Grant CE, Almquist KC, Stewart AJ, Kurz EU, Duncan AM and Deeley RG (1992) Overexpression of a transporter gene in a multidrug-resistant human lung cancer cell line. *Science* 258:1650-1654.

Cole SPC, Sparks KE, Fraser K, Loe DW, Grant CE, Wilson GM and Deeley RG (1994) Pharmacological characterization of multidrug resistant MRP-transfected human tumor cells. *Cancer Res* 54:5902-5910.

Conrad S, Kauffmann HM, Ito K, Leslie EM, Deeley RG, Schrenk D and Cole SPC (2002) A naturally occurring mutation in MRP1 results in a selective decrease in organic anion transport and in increased doxorubicin resistance. *Pharmacogenetics* 12:321-330.

Dawson RJP, Hollenstein K and Locher KP (2007) Uptake or extrusion: crystal structures of full ABC transporters suggest a common mechanism. *Mol Microbiol* 65:250-257.

Dawson RJP and Locher KP (2006) Structure of a bacterial multidrug ABC transporter. *Nature* 443:180-185.

Deeley RG, Westlake C and Cole SPC (2006) Transmembrane transport of endo- and xenobiotics by mammalian ATP-binding cassette multidrug resistance proteins. *Physiol Rev* 86:849-899.

Deeley RG and Cole SPC (2006) Substrate recognition and transport by multidrug resistance protein 1 (ABCC1) *FEBS Letters* 580:1103–1111

DeGorter MK, Conseil G, Deeley RG, Campbell RL and Cole SPC (2008) Molecular modeling of the human multidrug resistance protein 1 (MRP1/ABCC1). *Biochem Biophys Res Commun* 365:29-34.

Gao M, Cui HR, Loe DW, Grant CE, Almquist KC, Cole SPC and Deeley RG (2000) Comparison of the functional characteristics of the nucleotide binding domains of multidrug resistance protein 1. *J Biol Chem* 275:13098-13108.

Gao M, Loe DW, Grant CE, Cole SPC and Deeley RG (1996) Reconstitution of ATP-dependent leukotriene C_4 transport by co-expression of both half-molecules of human multidrug resistance protein in insect cells. *J Biol Chem* 271:27782-27787.

Grant CE, Valdimarsson G, Hipfner DR, Almquist KC, Cole SPC and Deeley RG (1994) Overexpression of multidrug resistance-associated protein (MRP) increases resistance to natural product drugs. *Cancer Res* 54:357-361.

Haimeur A, Conseil G, Deeley RG and Cole SPC (2004) Mutations of charged amino acids in or near the transmembrane helices of the second membrane spanning domain differentially affect the substrate specificity and transport activity of the multidrug resistance protein MRP1 (ABCC1). *Mol Pharmacol* 65:1375-1385.

Haimeur A, Deeley RG and Cole SPC (2002) Charged amino acids in the sixth transmembrane helix of multidrug resistance protein 1 (MRP1/ABCC1) are critical determinants of transport activity. *J Biol Chem* 277:41326-41333.

Hipfner DR, Almquist KC, Stride BD, Deeley RG and Cole SPC (1996) Location of a protease-hypersensitive region in the multidrug resistance protein (MRP) by mapping of the epitope of MRP-specific monoclonal antibody QCRL-1. *Cancer Res* 56:3307-3314.

Hirohashi T, Suzuki H, Takikawa H and Sugiyama Y (2000) ATP-dependent transport of bile salts by rat multidrug resistance-associated protein 3 (Mrp3). *J Biol Chem* 275:2905-2910.

Hooijberg JH, Broxterman HJ, Kool M, Assaraf YG, Peters GJ, Noordhuis P, Scheper RJ, Borst P, Pinedo HM and Jansen G (1999) Antifolate resistance mediated by the multidrug resistance proteins MRP1 and MRP2. *Cancer Res* 59:2532-2535.

Iliás A, Urbán Z, Seidl TL, Le Saux O, Sinkó E, Boyd CD, Sarkadi B and Váradi A. (2002) Loss of ATP-dependent transport activity in pseudoxanthoma elasticum-associated mutants of human ABCC6 (MRP6). *J Biol Chem* 277:16860-16867

Koike K, Conseil G, Leslie EM, Deeley RG and Cole SPC (2004) Identification of proline residues in the core cytoplasmic and transmembrane regions of multidrug resistance protein 1 (MRP1/ABCC1) important for transport function, substrate specificity, and nucleotide interactions. *J Biol Chem* 279:12325-12336.

Koike K, Oleschuk CJ, Haimeur A, Olsen SL, Deeley RG and Cole SPC (2002) Multiple membrane-associated tryptophan residues contribute to the transport activity and substrate specificity of the human multidrug resistance protein, MRP1. *J Biol Chem* 277:49495-49503.

Kool M, van der Linden M, de Haas M, Scheffer G, de Vree JM, Smith AJ, Jansen G, Peters GJ, Ponne N, Scheper R, Elferink.R.P., Baas F and Borst P (1999) MRP3, an organic anion transporter able to transport anti-cancer drugs. *Proc Natl Acad Sci USA* 96:6914-6919.

Leier I, Jedlitschky G, Buchholz U, Cole SPC, Deeley RG and Keppler D (1994) The MRP gene encodes an ATP-dependent export pump for leukotriene C_4 and structurally related conjugates. *J Biol Chem* 269:27807-27810.

Leier I, Jedlitschky G, Buchholz U, Center M, Cole SPC, Deeley RG and Keppler D (1996) ATP-dependent glutathione disulphide transport mediated by the MRP gene-encoded conjugate pump. *Biochem J* 314:433-437.

Leslie EM, Bowers RJ, Deeley RG and Cole SPC (2003) Structural requirements for functional interaction of glutathione tripeptide analogs with the human multidrug resistance protein 1 (MRP1). *J Pharmacol Exp Ther* 304:643-653.

Loe DW, Almquist KC, Cole SPC and Deeley RG (1996a) ATP-dependent 17 β-Estradiol 17-(β-D-glucuronide) transport by multidrug resistance protein (MRP). Inhibition by cholestatic steroids. *J Biol Chem* 271:9683-9689.

Loe DW, Almquist KC, Deeley RG and Cole SPC (1996b) Multidrug resistance protein (MRP)-mediated transport of leukotriene C_4 and chemotherapeutic agents in membrane vesicles. Demonstration of glutathione-dependent vincristine transport. *J Biol Chem* 271:9675-9682.

Loe DW, Deeley RG and Cole SPC (1998) Characterization of vincristine transport by the M(r) 190,000 multidrug resistance protein (MRP): evidence for co-transport with reduced glutathione. *Cancer Res* 58:5130-5136.

Qian YM, Grant CE, Westlake CJ, Zhang DW, Lander PA, Shepard RL, Dantzig AH, Cole SPC and Deeley RG (2002) Photolabeling of human and murine multidrug resistance protein 1 with the high affinity inhibitor [^{125}I]LY475776 and azidophenacyl-[^{35}S]glutathione. *J Biol Chem* 277:35225-35231.

Qian YM, Qiu W, Gao M, Westlake CJ, Cole SPC and Deeley RG (2001a) Characterization of binding of leukotriene C_4 by human multidrug resistance protein 1: evidence of differential interactions with NH2- and COOH-proximal halves of the protein. *J Biol Chem* 276:38636-38644.

Qian YM, Song WC, Cui H, Cole SPC and Deeley RG (2001b) Glutathione stimulates sulfated estrogen transport by multidrug resistance protein 1. *J Biol Chem* 276:6404-6411.

Rappa G, Lorico A, Flavell RA and Sartorelli AC (1997) Evidence that the multidrug resistance protein (MRP) functions as a co-transporter of glutathione and natural product toxins. *Cancer Res* 57:5232-5237.

Renes J, de Vries EG, Nienhuis EF, Jansen PL and Muller M (1999) ATP- and glutathione-dependent transport of chemotherapeutic drugs by the mutidrug resistance protein MRP1. *Br J Pharmacol* 126:681-688.

Rius M, Hummel-Eisenbeiss J and Keppler D (2008) ATP-dependent transport of leukotrienes B4 and C4 by the multidrug resistance protein ABCC4 (MRP4). *J Pharmacol Exp Ther*. 324, 86-94.

Sakamoto H, Hara H, Hirano K and Adach T (1999) Enhancement of glucuronosyl etoposide transport by glutathione in multidrug resistance-associated protein-overexpressing cells. *Cancer Lett* 135:113-119.

Westlake CJ, Qian YM, Gao M, Vasa M, Cole SPC and Deeley RG (2003) Identification of the structural and functional boundaries of the multidrug resistance protein 1 cytoplasmic loop 3. *Biochemistry* 42:14099-14113.

Zelcer N, Reid G, Wielinga P, Kuil A, van der Heijden I, Schuetz JD and Borst P (2003) Steroid and bile acid conjugates are substrates of human multidrug-resistance protein (MRP) 4 (ATP-binding cassette C_4). *Biochem J* 371:361-367.

Zelcer N, Saeki T, Reid G, Beijnen JH and Borst P (2001) Characterization of drug transport by the human multidrug resistance protein 3 (ABCC3). *J Biol Chem* 276:46400-46407.

Zeng H, Liu G, Rea PA and Kruh GD (2000) Transport of amphipathic anions by multidrug resistance protein 3. *Cancer Res* 60:4779-4784.

Zhang DW, Gu HM, Vasa M, Muredda M, Cole SPC and Deeley RG (2003) Characterization of the role of polar amino acid residues within predicted transmembrane helix 17 in determining the substrate specificity of multidrug resistance protein 3. *Biochemistry* 42:9989-10000.

Footnotes:

This work was supported by a grant from the Canadian Institutes of Health Research (CIHR) (MOP-62824).

[1]*Present Address: Gene Expression & Protein Biochemistry, Pharmaceutical Research Institute, Bristol-Myers Squibb Company, P.O. Box 4000, H12-03, Princeton, NJ 08543, USA (M.G.)*

[2]*Present Address: University of Western Ontario, London, ON N6A 5B8, Canada (M.K.D.)*

Legends for Figures

Fig. 1. Predicted topology of human MRP1 and location of the MRP3 segments that were exchanged in the MRP1/MRP3 hybrid proteins. (A) The predicted topology of human MRP1 with 17 transmembrane (TM) helices, organized into 3 membrane spanning domains (MSDs), and 2 nucleotide binding domains (NBDs). Also depicted is the site of division of the protein used for expression as 2 half molecules, $MRP1_{1-932}$ and $MRP1_{932-1531}$. (B) Portions of MSD1 and MSD2 of MRP1 that were exchanged for the equivalent regions of MRP3 (fragments A-L) and expressed as MRP1/MRP3 hybrid proteins in the Sf21 expression system, as described in the text. (C-D) ATP-dependent LTC_4 (C) and $E_2$17ßG (D) Transport by membrane vesicles expressing wild-type MRP1 (dh), the $MRP1_{1-425}MRP3_{411-502}MRP1_{517-1531}$ hybrid protein (G) and vesicles expressing a control protein ß-glucosidase (ß-gus). Shown are transport levels obtained at 2 min for LTC_4 and at 3 min for $E_2$17ßG. Conditions used for the transport assays were as described in Materials and Methods. The results shown are the averages and standard deviations of triplicate assays from a typical experiment. Similar results were obtained with a second set of independently produced membrane vesicle preparations.

Fig. 2. Partial sequence alignment and ATP-dependent [^{3}H]LTC_4 and [^{3}H]$E_2$17βG uptake by membrane vesicles containing wild-type MRP1 or MRP1/MRP3 hybrid proteins G1 and G2. (A) Upper panel: Sequence alignment of the 'G' region of human MRP1 (amino acids 425-516) and the corresponding region of MRP3 (amino acids 411-502). The corresponding region of MRP3 was determined by aligning the amino acid sequences of all ABCC family members. In the alignment shown, identical residues are indicated by colons while residues that differ between

MRP1 and MRP3 are in boldface type. The sequences of the G1 and G2 regions are depicted on separate lines of the figure. Lower panel: Sequence alignment of the regions of all MRPs corresponding to amino acids 425 to 463 of MRP1 generated as decribed above. Critical residues described in the text are underlined. (B) Immunoblot of an SDS-PAGE gel loaded with 1 µg total membrane vesicle protein per lane from Sf21 cells expressing wild type or G1 and G2 hybrid proteins probed with mAb MRPr1 or MRPm6 which recognize the NH_2-terminal fragment, amino acids 1-932, and the COOH-terminal fragment, amino acids 932-1531, of MRP1, respectively. Densitometry of the blot indicated that levels of the hybrid proteins were very similar to that of wild-type MRP. The procedures used for immunoblotting and densitometry were as described in Materials and Methods. Consequently, no adjustment of [^{3}H]LTC_4 and [^{3}H]$E_2$17βG uptake to compensate for differences in expression was done. (C-D) ATP-dependent uptake of [^{3}H]LTC_4 (50 nM, 23°C, 3 min) and [^{3}H]$E_2$17βG (400 nM, 37°C, 5 min). The results shown are the means ± SD of triplicate determinations in a single experiment. Similar results were obtained with a second set of independently produced membrane vesicle preparations.

Fig. 3. ATP-dependent uptake of [^{3}H]labeled LTC_4, $E_2$17ßG, $E_1$3SO_4 and MTX by membrane vesicles prepared from Sf21 cells infected with virus encoding wild-type or mutant MRP1. (A) Levels of wild-type and mutant MRP1 proteins were determined by transferring vesicle protein to membranes using a slot blot apparatus, followed by sequential detection with mAbs QCRL1 and MRPm6, and densitometry, as described in *Materials and Methods.* Shown are scans of 1 µg samples only. Not shown are scans of the 0.5, 1.5 and 2 µg protein samples. The numbers below the blots refer to the levels of mutant MRP1 proteins relative to the level of the wild-type protein (dh), as determined by densitometry. (B-E) ATP-dependent uptake of: (B) [^{3}H]LTC_4, measured

for 2 min; (C) [^{3}H]$E_2$17βG measured for 3 min; (D) [^{3}H]$E_1$3SO_4 measured with the addition of 2 mM S-methyl GSH for 1 min; (E) [^{3}H]MTX measured for 20 min. The relative levels of protein expression determined by densitometry (A) were used to normalize transport data to the expression level of wild-type MRP1. Values are means ± SD of 3 determinations in a single experiment. Similar results were obtained with 2 or more independently produced membrane vesicle preparations.

Fig. 4. Kinetic analysis of ATP-dependent [^{3}H]LTC_4 uptake by wild-type and mutant MRP1 proteins expressed in Sf21 cells. (A) Time course of ATP-dependent [^{3}H]LTC_4 uptake by membrane vesicles was measured at various LTC_4 concentrations (25 nM-1 μM) for 1 min at 23°C. (B) Hanes-Wolff plot of the data shown in (A). Shown are wild-type MRP1 (■), Y440F (▲), I441L (▼), Y440F/I441L (♦). Values are mean ± SD of triplicate determinations in single experiments. Kinetic parameters were determined from linear regression analysis of Hanes-Wolff plots of [S]/V *vs* [S].

Fig. 5. [^{3}H]LTC_4 photolabeling of membrane vesicle isolated from Sf21 cells expressing wild-type and mutant MRP1 proteins. (A) Immunoblot showing the relative amounts of MRP1 protein in each sample after adjustment for relative MRP1 protein expression; wild-type MRP1 (35 μg) and mutants Y440F (75 μg), I441L (22 μg) and Y440F/I441L (20 μg). (B) [^{3}H]LTC_4 photolabeling of wild-type and mutant MRP1 proteins. Each sample was adjusted to a total of 75 μg of protein with membrane vesicles from Sf21 cells expressing ß-gus. The NH_2- and COOH-proximal half molecules are indicated as as N- and C-half, respectively. The numbers below the

blots refer to the levels of mutant MRP1 proteins relative to the level of the wild-type protein (dh), as determined by densitometry.

Fig. 6. ATP-dependent uptake of [^{3}H]LTC$_4$ and [^{3}H]E$_2$17ßG by Sf21 membrane vesicles containing wild-type and Tyr^{440} mutant MRP1proteins. (A) [^{3}H]LTC$_4$ uptake measured at 2 min. (B) [^{3}H]E$_2$17ßG uptake measured at 3 min. Values were normalized to account for differences in for MRP1 protein expression levels. Values are mean ± SD of 3 determinations in a single experiment. Similar results were obtained with 2 independently produced membrane vesicle preparations.

Fig. 7. S-methyl GSH-enhanced ATP-dependent [^{3}H]E$_1$3SO$_4$ uptake and azidophenacyl-[^{35}S]GSH photolabeling of wild-type and mutant MRP1 proteins. (A) ATP-dependent [^{3}H]E$_1$3SO$_4$ uptake by membrane vesicles prepared from Sf21 cells was measured at various concentrations of [^{3}H]E$_1$3SO$_4$ (3-20 µM) in the presence of 2 mM S-methyl GSH. Uptake was measured after a 30 sec incubation at 37^{o}C. Data points are the means ± S.D. of triplicate determinations in a single experiment and uptake levels have been adjusted to compensate for differences in the relative levels of mutant proteins relative to wild-type MRP1. (B-C) For photolabeling with azidophenacyl-[^{35}S]GSH, membrane vesicles prepared from stably transfected HEK293 cells were incubated with azido phenacyl-[^{35}S]GSH (0.3 µCi) and processed as described in *Materials and Methods*. For each sample, approximately 120 µg of total membrane protein was analysed but amounts of the specific membrane vesicle preparations were adjusted to compensate for the relative MRP1 protein expression by the addition of membrane vesicles isolated from HEK293 cells stably transfected with empty expression vector, PC7. (B)

The immunoblot analysis with mAb MRP1m6 of the proteins. The numbers below the blots refer to the levels of mutant MRP1 proteins relative to the level of the wild-type protein, as determined by densitometry. (C) Photolabeling of the remaining sample from (B) with azidophenacyl-[^{35}S]GSH.

Fig. 8. The figure illustrates three views of the model of MRP1 based on the crystal structure of the ADP bound form of *S. Aureus* Sav1866 generated as described (DeGorter et al., 2008) and produced using PyMol (DeLano Scientific LLC, San Carlos, CA). The locations of residues in TMs 6 and 8 referred to in the text, which have been shown to selectively influence transport of LTC_4, are indicated. (A) View of MRP1 from the extracellular face of the membrane to illustrate the disposition of residue side chains relative to the putative translocation pore. (B) View of MRP1 positioned to illustrate the tilt and curvature of TMs 6 and 8. (C) View of MRP1 from the plane of the membrane illustrating the positions of TMs 6, 7 and 8 and coupling helix 1 in MSD1 (shown in pale purple) which links TMs 7 and 8 and sits at the interface between the two NBDs.

Table 1: MRP1 dh constructs containing multiple mutations from the G region

Mutant #	Mutations Included
23	M443L/Y440F/1441L
24	A481G/V482A/M483V/M485V
25	V479L/A481G/V482A/M483V/M485V
26	A493K/H494Q/S497L/N500S
27	V479L/A481G/V482A/M483V/M485V
28	V479L/A481G/V482A/M483V/N500S
29	A493K/H494Q/S497L/N500S/N506S
30	A493K/H494Q/S497L/N506S/T487M/K488R/T489A/Y490F

To generate the vectors expressing the mutant MRP1 proteins, site-directed mutagenesis was performed using the QuikChange® II Site-Directed Mutagenesis Kit (Stratagene, La Jolla, CA), as described in Materials and Methods. Each construct was verified to be correct by both sequencing and restriction enzyme analysis.

Table 2: Relative Drug Resistance of HEK293 Cells Transfected with Wild-type and Mutant MRP1[a]

Transfectant	Drug (relative resistance factor[a])		
	Vincristine	**VP-16**	**Doxorubicin**
HEKMRP1	15.6 ± 2.5	16.2 ± 4.9	4.5 ± 0.3
HEKMRP1-Y440F	2.4 ± 0.5	2.7 ± 0.8	1.3 ± 0.2
	(5.1)	(6.0)	(1.9)
HEKMRP1-1441L	8.9 ± 2.5	4.1 ± 1.2	3.7 ± 1.4
	(9.7)	(4.4)	(4.1)
HEKMRP1-M443L	6.5 ± 1.2	5.8 ± 0.5	3.8 ± 0.7
	(6.0)	(5.4)	(3.6)
HEKMRP1-Y440F/1441L	3.9 ± 1.0	1.3 ± 0.3	1.2 ± 0.2
	(7.5)	(1.7)	(1.5)
HEKMRP3	1.1 ± 0.1	6.4 ± 1.9	0.87 ± 0.2

[a]The relative resistance factor was obtained by dividing the IC_{50} values for the wild-type or mutant MRP1-transfected cells by the IC_{50} value for cells transfected with the expression vector alone. Each value represents the mean ± SD of 3 or more independent experiments. Resistance factors normalized for differences in MRP1 protein expression are indicated in parenthesis.

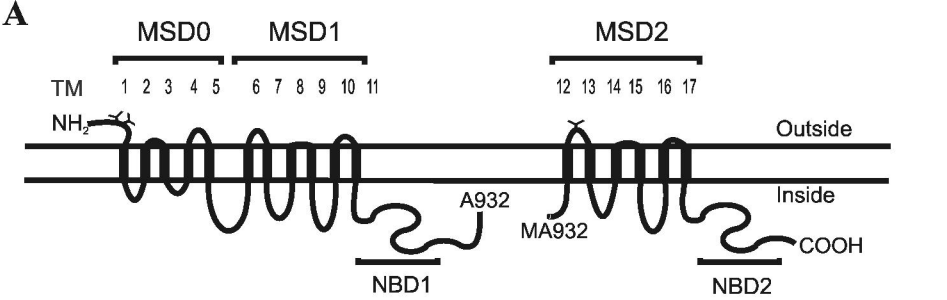

B MRP1/3 Hybrid Constructs:

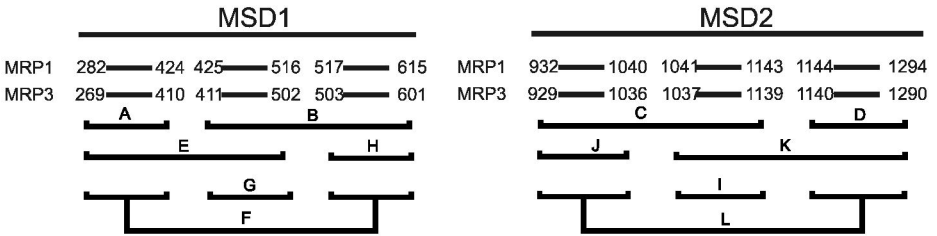

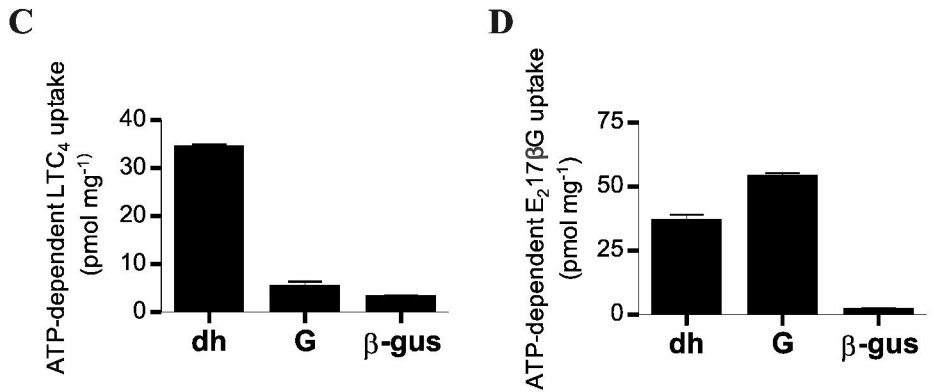

Figure 1

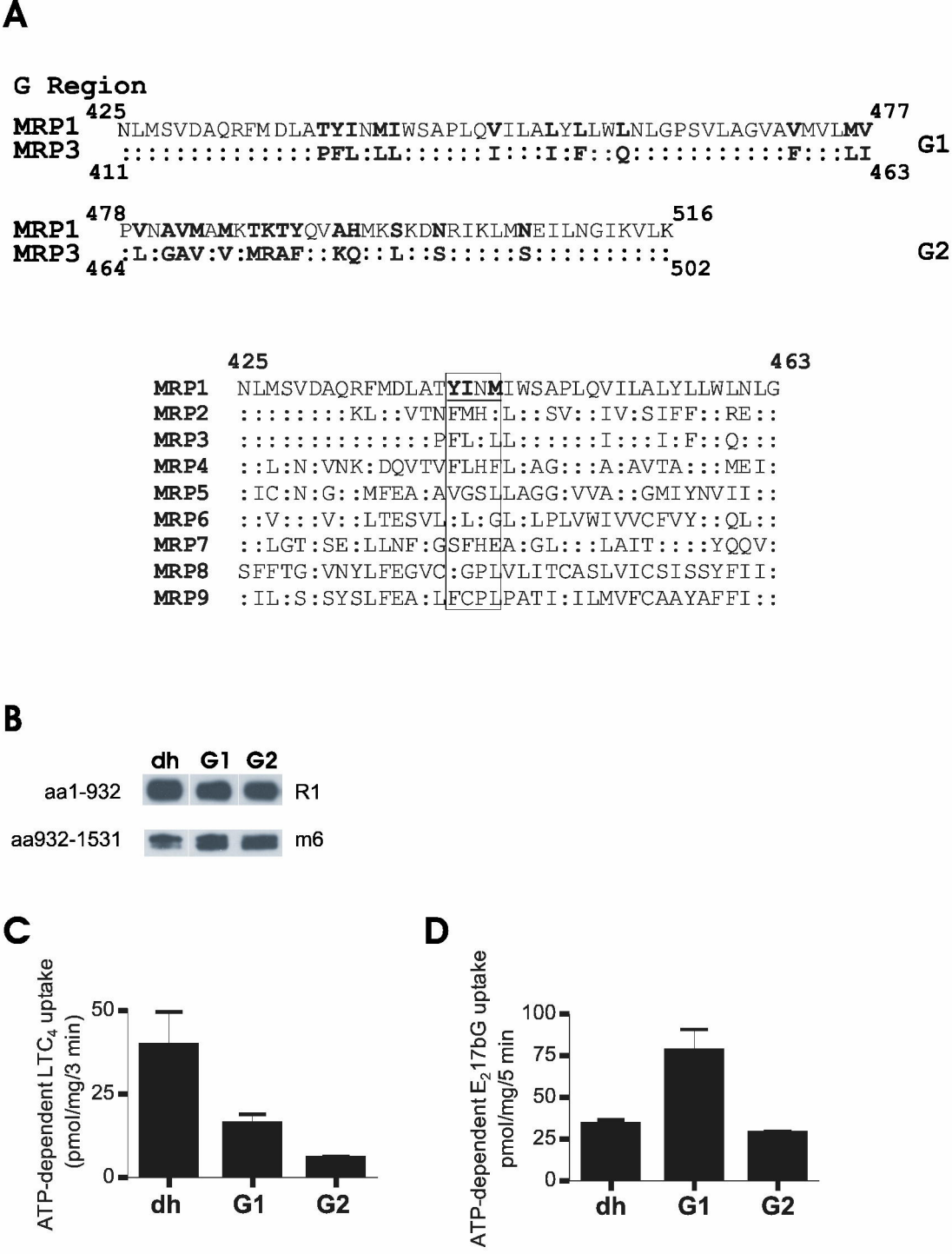

Figure 2

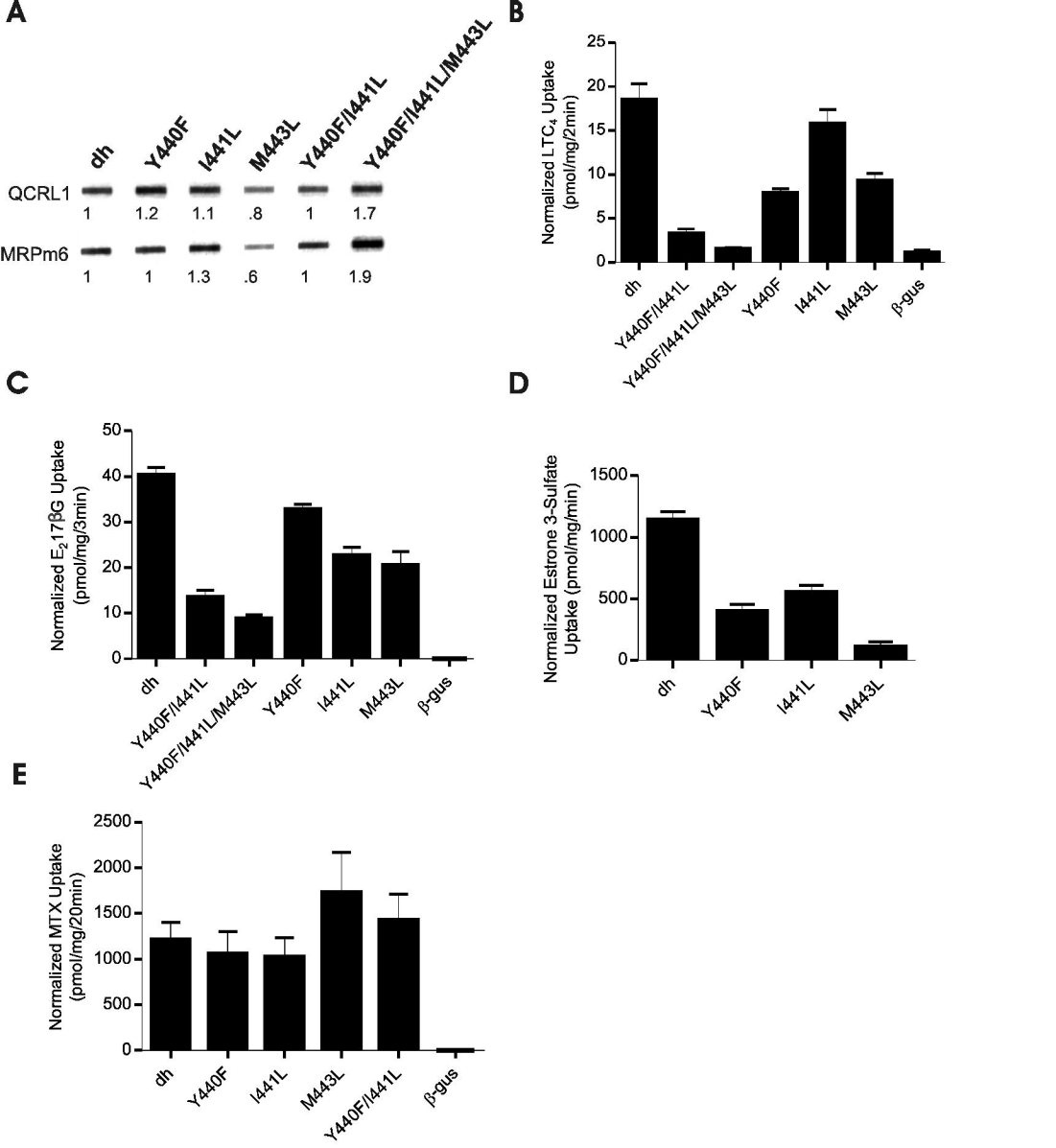
A
dh
Y440F
I441L
M443L
Y440F/I441L
Y440F/I441L/M443L
QCRL1
1
1.2
1.1
.8
1
1.7
MRPm6
1
1
1.3
.6
1
1.9
B
Normalized LTC4 Uptake (pmol/mg/2min)
25
20
15
10
5
0
dh
Y440F/I441L
Y440F/I441L/M443L
Y440F
I441L
M443L
β-gus
C
Normalized E2 17βG Uptake (pmol/mg/3min)
50
40
30
20
10
0
dh
Y440F/I441L
Y440F/I441L/M443L
Y440F
I441L
M443L
β-gus
D
Normalized Estrone 3-Sulfate Uptake (pmol/mg/min)
1500
1000
500
0
dh
Y440F
I441L
M443L
E
Normalized MTX Uptake (pmol/mg/20min)
2500
2000
1500
1000
500
0
dh
Y440F
I441L
M443L
Y440F/I441L
β-gus

Figure 3

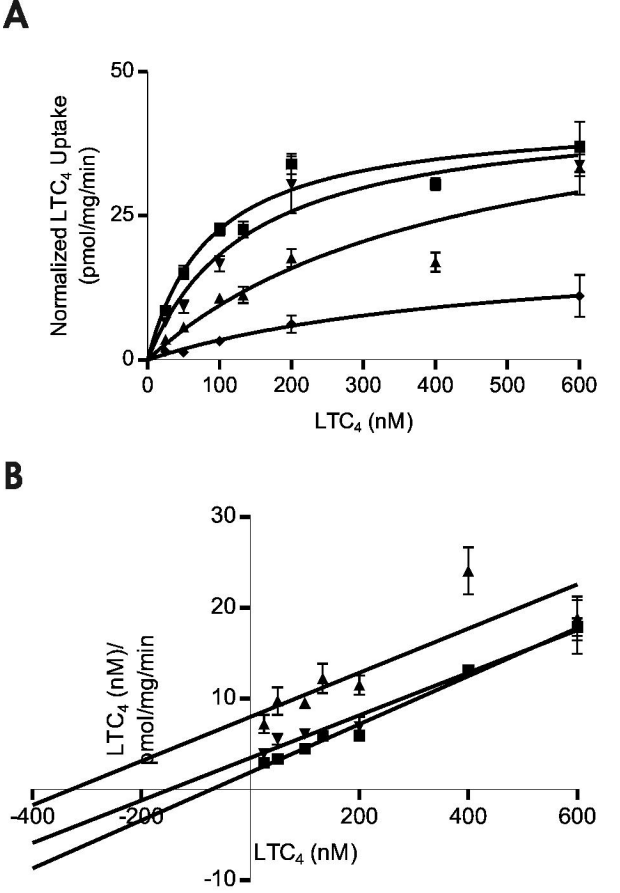
A
Normalized LTC4 Uptake
(pmol/mg/min)
50
25
0
0
100
200
300
400
500
600
LTC4 (nM)
B
LTC4 (nM)/
pmol/mg/min
30
20
10
-10
-400
-200
200
400
600
LTC4 (nM)

Figure 4

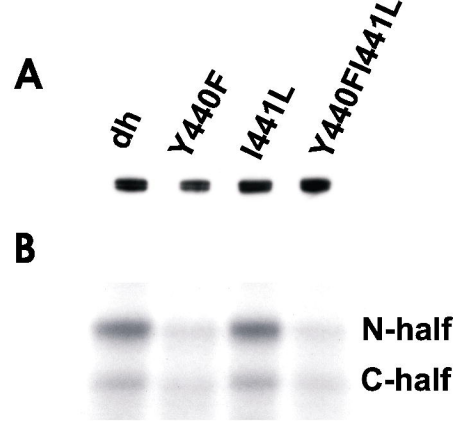

Figure 5

A

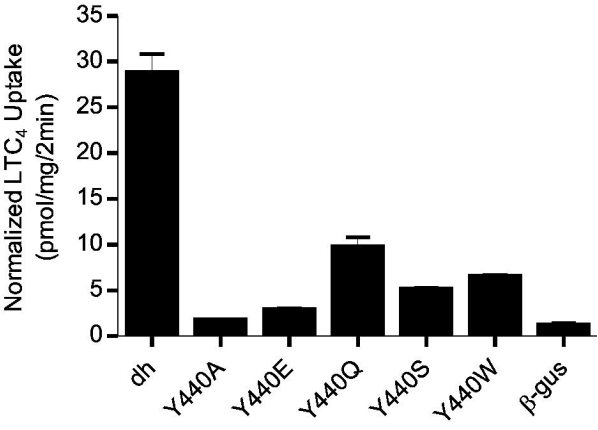
Normalized LTC4 Uptake
(pmol/mg/2min)
35
30
25
20
15
10
5
0
dh
Y440A
Y440E
Y440Q
Y440S
Y440W
β-gus

B

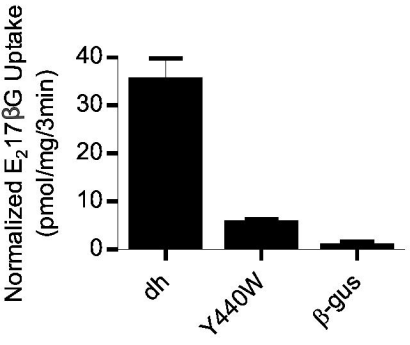
Normalized E2 17βG Uptake
(pmol/mg/3min)
40
30
20
10
0
dh
Y440W
β-gus

Figure 6

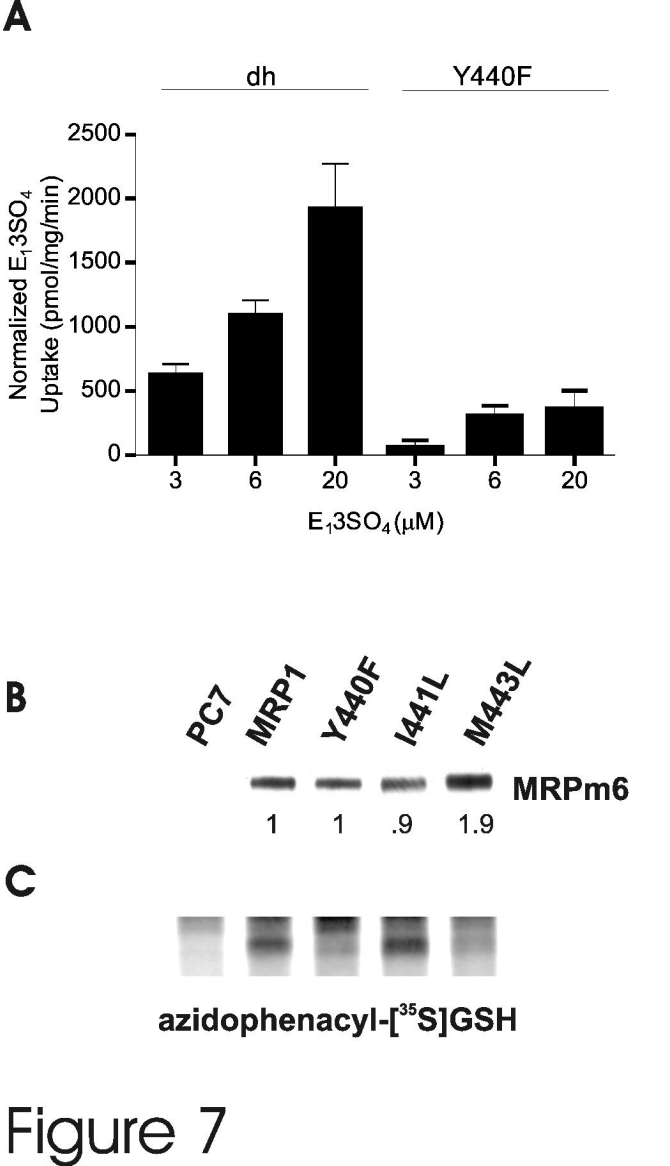
A
dh
Y440F
2500
2000
1500
1000
500
0
Normalized E1 3SO4 Uptake (pmol/mg/min)
3
6
20
3
6
20
E1 3SO4 (μM)
B
PC7
MRP1
Y440F
I441L
M443L
MRPm6
1
1
.9
1.9
C
azidophenacyl-[35S]GSH

Figure 7

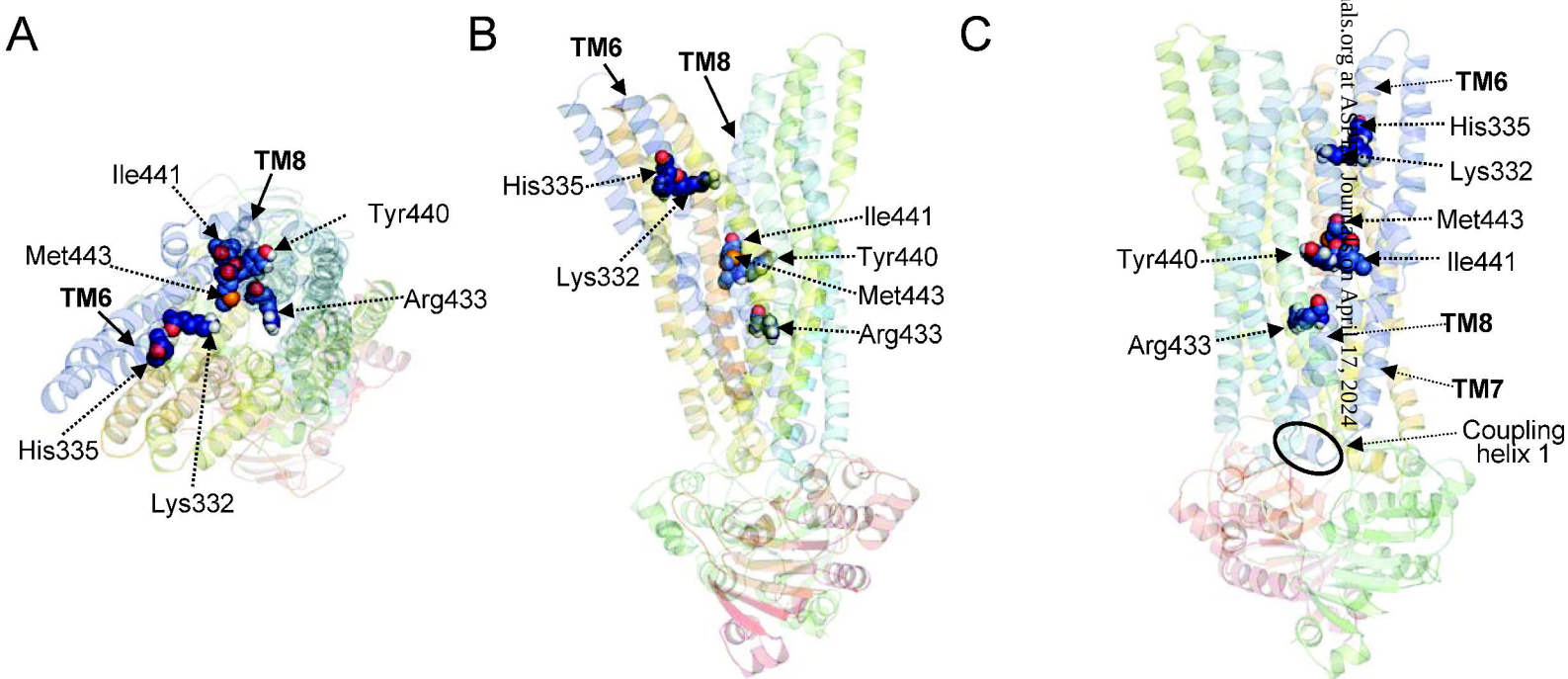

Fig.8